Supplementary Information (SI) for New Journal of Chemistry.

Supporting information

Zinc Ferrite as a Sustainable and Robust catalyst for Suzuki-Miyaura Cross-Coupling reaction: An Experimental and Theoretical Analysis

Amar Jyoti Kalita, Aquif Suleman, Tikendrajit Chetia, Raktim Nath, Rahul Kar, Bolin Chetia*

Department of Chemistry, Dibrugarh University, Dibrugarh (Assam), 786004.
Corresponding author: Prof. Bolin Chetia

E-mail : bolinchetia@dibru.ac.in

Tel: +91 9957047139

Table of Contents

1.Table S1: d-spacing calculation of $ZnFe_2O_4$ NPs from SAED pattern:

Sl no.	1/2r (nm^{-1})	1/r (nm^{-1})	r (nm)	d-spacing (Å)	(h k l)
1	10.966	5.483	0.182382	1.823819077	(4 2 2)
2	12.159	6.0795	0.164487	1.644872111	(5 1 1)
3	8.594	4.297	0.232721	2.327205027	(2 2 2)
4	7.111	3.5555	0.281254	2.812543946	(3 1 1)
5	13.977	6.9885	0.143092	1.430922229	(4 4 0)
6	17.1	8.55	0.116959	1.169590643	(5 3 3)
7	6.175	3.0875	0.323887	3.238866397	(2 2 0)

2.Figure S1: IR spectra of $ZnFe_2O_4$

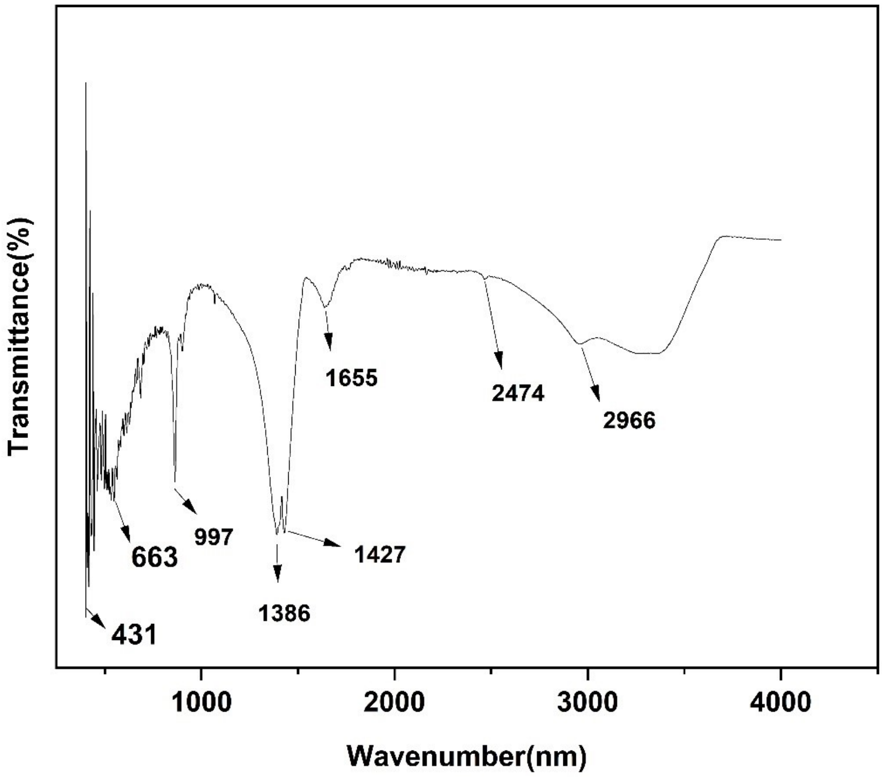

Figure 1 depicts the FT-IR spectrum of a $ZnFe_2O_4$ sample, demonstrating how radiation transmittance (%) varies with spectroscopic wave number ($\bar{\nu}$), which signifies the irradiation energy. There are basically two regions in the spectrum that can be broadly categorized. The first region comprises high-energy lattice vibrations in metal oxides, while the second comprises low-energy vibrations in organic functional group bonds. The 431 and 663 cm^{-1} transmittance bands result from vibrations in the oxide ion's lattice in response to heavy metal cations. Two bands 2474 & 2966 Cm^{-1} were observed on $ZnFe_2O_4$ nanoparticles formed from an OA $-CH_2$ organic group stretching in asymmetric and symmetric modes. The peak at 1655 cm^{-1} corresponds to C–O stretching. The peak at 1427 cm^{-1} may be due to the symmetric stretching mode of COO^-. The stretching mode of C–H is responsible for the band at 1386 cm^{-1}, whereas the C–N stretching mode could be the source of the peak at 997 cm^{-1}. A lower frequency region was assigned to the absorption peaks of $-CH_2$.

3.Table S2: ICP-MS result

Sl. No.	Sample Name	56Fe	64Zn
1	$ZnFe_2O_4$	**21.385**	**1.843**
Unit		**%**	**%**
Detection Limit in ppm		**0.01**	**0.10**

4.Catalyst leaching and recyclability test

Hot filtration test: A hot filtration test was conducted for the reaction to determine whether the catalyst behaved homogeneously or heterogeneously. Using Fluorobenzene (0.15 mmol) and phenyl boronic acid (0.15 mmol) with the standard optimized reaction conditions at 60 °C, the reaction progress was monitored via TLC. An external magnet extracted the catalyst after 50% conversion (4 h). With the filtrate, the reaction was continued for 4 hours. In contrast, no cross-coupling products were formed. The catalyst was therefore ruled out to be semi-heterogeneous or homogeneous.

Recyclability: A recyclability test was conducted on the catalyst during the reaction. An external magnet separated the catalyst after the reaction was completed. The catalyst was then thoroughly washed with EtOH and deionized water and dried at 40°C before being used in a second batch of reactions. This study demonstrated that catalysts can be recycled and reused up to a fifth cycle without a reduction in catalytic activity or product yield. The reaction recyclability with recovered catalyst in mol% after each catalytic cycle is shown in Fig (c) below.

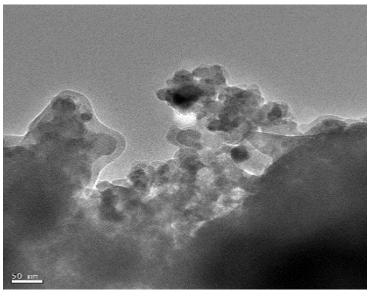

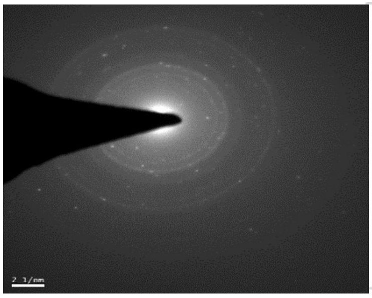

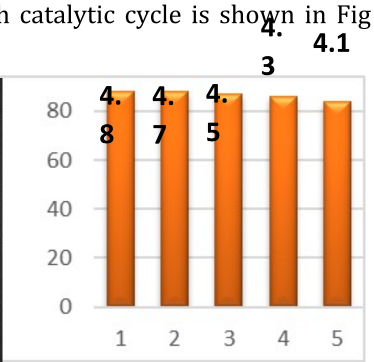

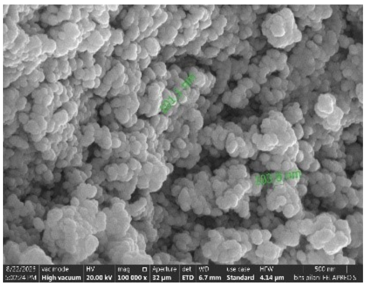

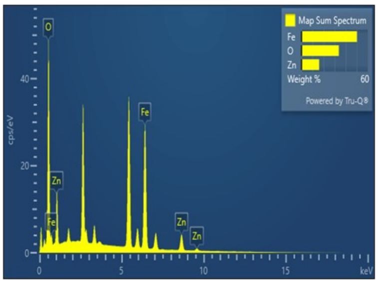

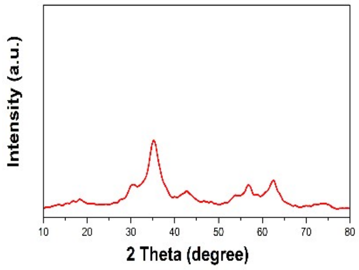

Figure S2: (a,b) TEM image of the recycled catalyst after 5th cycle. (c) Recyclability of $ZnFe_2O_4$ MNPs.

(e,f) SEM and EDX image of recyclable catalyst after 5th cycle respectively. (g)PXRD of Catalyst after 5th cycle.

5.Table S3: Comparison Table for Recently Reported Works on Suzuki–Miyaura cross-coupling reaction of various fluoro compounds

Sl no.	Fluoro compound	Catalyst	Condition	Time (h)	Yield (%)	References
1	Aryl fluorosulfates(1mmol)	$Pd(OAc)_2$ (1 mol%)	Et_3N (3 equiv.), H_2O , r.t.	10	89	16
2	4-fluoro-bromobenzene(1mmol)	$Pd_3(OAc)_6/6PPh_3$	nBu_4NOH (2.5 equiv.) THF H_2O (1:1 v/v, 0.2 M), 40 °C, N_2	4	82	17
3	Aryl fluorosulphates (0.15 mmol)	$Pd(OAc)_2$ (1 mol%)	PPh_3 (2.5 mol%), Net3, 1,4-dioxane/H_2O, 60°C	12	88	18
4	Aryl fluorides (0.30 mmol)	$NiCl_2(PCy_3)_2$ (0.015 mmol)	K_3PO_4 (1.4 mmol), and toluene (0.90 mL), 120 °C	12	52	19
5	Alkyl Fluorides (0.2 mmol)	$Ni(cod)_2$ (5 mol %)	LiI (0.3 mmol), and Cs_2CO_3 (0.4 mmol), dry toluene (2ml), 100 °C	48	71	20
6	**Aryl fluorides (0.15mmol)**	**$ZnFe_2O_4$ (5 mol %)**	**TEA (0.45mmol), Ethanol (3 ml), 60°C**	**8**	**88**	**this work**

Reaction conditions: 0.15 mmol reactant 1, 0.15 mmol reactant 2 and 0.45 mmol TEA were reacted in 3 ml ethanol at 60°C for 8 hrs with 5 mol% of $ZnFe_2O_4$ catalyst.

6.Table S4: ICP-MS result of recycled catalyst:

Sl. No.	Sample Name	*56Fe	*64Zn
1	**AK1**	**5.28**	**0.40**
Unit		**ppm**	**ppm**
Detection Limit in ppm		**0.01**	**0.01**

7.E-factor calculation for the synthesis of biphenyl (Scheme 1, entry 1):

Substrate: Phenylboronic acid (0.15 mmol) = 0.0182 g

Fluorobenzene (0.15 mmol) = 0.0144 g

Catalyst: $ZnFe_2O_4$ = 0.0120 g

Solvent: EtOH (3 mL) = 2.367 g

Wash solvent (ethyl acetate + H_2O) = 5.70 g

Product: Biphenyl (Entry 1) = 0.0185 g

$$\textbf{E factor} = \frac{\textbf{mass used − mass recovered}}{\textbf{mass of product}}$$

$$\text{E factor} = \frac{(0.0182+0.0144+0.0120+2.367+5.70) - (5.70+2.367+0.0120+0.0185)}{0.0185}$$

E factor = 0.762 g

Table S5. Calculation of E-factor values for some of the synthesized substituted biphenyl

Entry	E-factor (g)	Entry	E-factor (g)
2	0.370	16	0.419
3	0.418	17	0.341
4	0.474	18	0.131
5	0.622	19	0.231
6	0.535	20	0.157
7	0.813	21	0.282
8	0.804	22	0.951
9	1.02	23	0.975
10	0.753	24	0.407
11	0.171	25	0.672
12	0.159	26	0.733
13	0.271		
14	0.197		
15	0.321		

8.Reaction mass efficiency (RME)

RME = mass of product /Σ(mass of stoichiometic reactants) × 100

Higher value measures **greenness** of a reaction

RME calculation for **Scheme 2, Entry 1:**

$$\text{RME} = \frac{0.0185}{0.0182+0.0144} \times 100$$

RME =56.74% (>55%, moderately sustainable)

9.Table S6: E-factor calculation for the synthesis of $ZnFe_2O_4$

Reactants	Amount (g)
$Zn(OAc)_2.6H_2O$	0.200
$FeCl_3$	0.295
NaOH	0.2
Water	20

Wash Solvents	24
Water recovered	20
Wash Solvent recover	24
Mass of $ZnFe_2O_4$ obtained	0.397

$$\text{E-factor} = \frac{(0.200+0.295+0.2+20+24) - (20+24+0.397)}{0.397}$$

$$= 0.750\text{g}$$

10.Table S7: E factor and RME for recent catalytic systems for the Suzuki– Miyaura coupling in aqueous media

	Bhalla et al. [32]	**Khan et al.** [33]	**S. Fortun et al.** [34]	**Our work**
E-Factor	>2232.6	32.95	30.35	0.1-0.9
RME	Not reported	Not reported	Not reported	55-98%

11. Principles of green chemistry

- **Principle 5**: Safer solvents and auxiliaries: Water and ethanol are used as solvent during the catalyst synthesis process, which are safer solvents and are easy to handle. Hence follows the green chemistry principle.
- **Principle 8**: Reduce derivatives: No unnecessary derivatization/reagents/blocking groups are used during the synthesis protocol; hence no additional steps required. The synthetic procedure was straight-forward and easy to carry out.
- **Principle 9**: Catalysis: The synthesized catalyst is highly catalytically active and superior to stoichiometric reagents.
- **Principle 12**: Inherently safer chemistry for accident prevention: All the substances/reagents used in the synthesis process are safe to use and free from any chemical explosion and fire.

12. Table S8. Radical scavenger experiments using $ZnFe_2O_4$ as catalyst at room temperature.

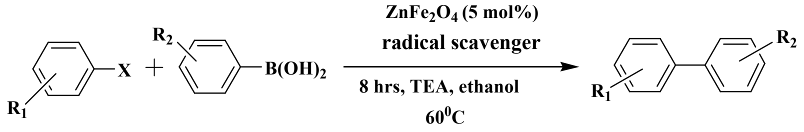

Sl. No.	Radical scavenger	Yield
1	-	80
2	TBA	45

3	TEMPO	25
4	BHT	trace

Reaction conditions: 0.15 mmol reactant 1, 0.15 mmol reactant 2 and 0.45 mmol TEA were reacted in 3 ml ethanol with radical scavenger (0.30 mmol) at 60ºC for 8 hrs with 5 mol% of $ZnFe_2O_4$ catalyst.

13.Copies of ^{1}H and ^{13}C NMR spectra (all products are purified by column chromatography)

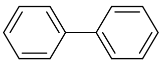

Biphenyl

^{1}H NMR (500 MHz, $CDCl_3$) δ 7.69 (d, 4H), 7.53 (t, *J* = 7.6 Hz, 4H), 7.44 (t, *J* = 7.3 Hz, 2H).

^{13}C NMR (125 MHz, $CDCl_3$) δ 141.35, 128.84, 127.34.

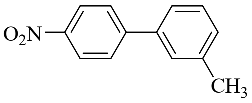

3-Methyl-4′-nitro-biphenyl

^{1}H NMR (500 MHz, $CDCl_3$) δ 8.28 (d, *J* = 8.1, 5.8 Hz, 2H), 8.27 (d, 2H), 7.28 (t,1H), 7.24 (d,1H), 7.22(d, 1H), 7.21 (s, 1H), 2.08 (s, 3H).

^{13}C NMR (125 MHz, $CDCl_3$) δ 167.77, 165.04, 126.38, 126.30, 116.52, 116.33, 77.34, 77.09, 76.83, 31.59.

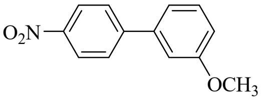

3-Methoxy-4′-nitro-biphenyl

^{1}H NMR (500 MHz, $CDCl_3$) δ 8.28 (d, *J* = 9.2, 4.7 Hz, 2H), 8.25 (d, *J* = 22.7, 15.0 Hz, 2H), 7.21 (s,1H), 7.22(d,1H), 7.25 (t, 1H), 7.29 (d, 1H), 3.52 (s, 3H).

^{13}C NMR (125 MHz, $CDCl_3$) δ 207.04, 165.05, 126.55, 116.08, 76.82, 30.93.

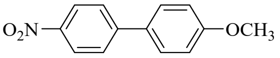

4-Methoxy-4′-nitro-biphenyl

^{1}H NMR (500 MHz, CDCl$_3$) δ 8.38 (d, *J* = 9.2, 4.7 Hz, 2H), 7.78 (d, 2H), 7.28 (d, 2H), 7.03 (d,2H), 3.90 (s, 3H).

^{13}C NMR (125 MHz, CDCl$_3$) δ 163.31, 137.66, 136.22, 113.52, 77.20, 76.82, 76.72 – 76.53, 55.24, 40.64.

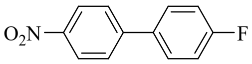

4′-Fluoro-4-nitro-biphenyl

^{1}H NMR (500 MHz, CDCl$_3$) δ 8.16 (d, 2H), 7.90 (d, 2H), 7.34 (d, 2H), 7.13 (d, 2H)

^{13}C NMR (125 MHz, CDCl$_3$) δ 167.33, 144.28, 136.23, 134.87, 127.27, 117.16.

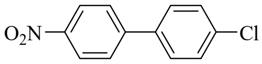

4′-Chloro-4-nitro-biphenyl

^{1}H NMR (500 MHz, CDCl$_3$) δ 8.19-8.17 (m, 2H), 7.97 (d, *J* = 8.1 Hz, 2H), 7.45 – 7.22 (m, 2H), 7.13 (d, *J* = 9.1 Hz, 2H).

^{13}C NMR (125 MHz, CDCl$_3$) δ 135.43, 135.29, 128.01, 126.33, 125.77 – 123.55, 117.16, 116.40 – 116.21, 77.89.

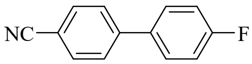

4′-Fluoro-biphenyl-4-carbonitrile

^{1}H NMR (500 MHz, CDCl$_3$) δ 7.72 (d, *J* = 16.6 Hz, 2H), 7.69 (d, 2H), 7.33 – 7.14 (m, 4H).

^{13}C NMR (125 MHz, CDCl$_3$) δ 164.07, 136.96, 134.86 – 134.67, 133.17, 118.13, 117.33, 116.82.

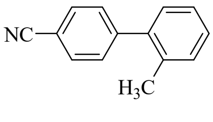

2′-Methyl-biphenyl-4-carbonitrile

^{1}H NMR (500 MHz, CDCl$_3$) δ 8.24 (d, *J* = 7.2 Hz, 2H), 7.92 (d, 2H), 7.48 (t, *J* = 7.3 Hz, 2H), 7.32 (d, *J* = 15.0, 7.4 Hz, 2H), 7.28 (d,2H), 2.85 (s, 3H).

^{13}C NMR (125 MHz, $CDCl_3$) δ 146.21, 137.19, 135.33, 132.13, 130.58, 125.18, 124.63, 78.14, 76.78, 23.00.

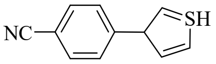

4-(-3*H*-1λ^4-Thiophen-3-yl)-benzonitrile

^1H NMR (500 MHz, $CDCl_3$) δ 7.93 (d, 2H), 7.28 (d, 2H), 7.15 (d, 2H), 6.78 (s,1H).

^{13}C NMR (125 MHz, $CDCl_3$) δ 77.29, 77.04, 76.78, 41.03, 30.01.

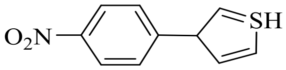

3-(4-Nitro-phenyl)-3*H*-1λ^4-thiophene

^1H NMR (500 MHz, $CDCl_3$) δ 7.93 (d, 2H), 7.37 (d, 2H), 7.28 (d, 2H), 6.89 (s,1H).

^{13}C NMR (125 MHz, $CDCl_3$) δ 77.29, 77.03, 76.78, 45.84, 8.59.

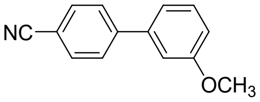

3-Methoxy-4′-benzonitrile

^1H NMR (500 MHz, $CDCl_3$) δ 7.60 (d, J = 8.4 Hz, 2H), 7.47 (d, 2H), 7.39 (s, 2H), 7.33 (d, 2H), 7.27 (d, 2H), 3.83 (s, 3H).

^{13}C NMR (126 MHz, $CDCl_3$) δ 139.71 – 139.55, 133.40, 129.72, 110.83, 77.29, 77.04, 76.78.

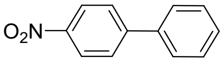

4-nitro-1,1′-biphenyl

^1H NMR (500 MHz, $CDCl_3$) δ 8.45 (d, 2H), 7.76 (d, J = 41.2 Hz, 2H), 7.70 (d, 2H), 7.52 (t, 2H), 4.5 (t, 1H).

^{13}C NMR (126 MHz, $CDCl_3$) δ 134.73, 133.59, 130.43, 123.94, 121.79.

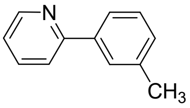

2-(m-tolyl) pyridine

^1H NMR (500 MHz, $CDCl_3$) δ 8.45 (d, 1H), 7.76 (t, 1H), 7.70 (d, 1H), 7.41 (d, 1H), 7.35 (d, 1H), 7.23 (t,1H), 7.15 (d, 2H), 2.87 (s, 3H).

^{13}C NMR (126 MHz, $CDCl_3$) δ 137.21, 127.81, 77.30, 77.04, 76.79, 45.73, 21.54, 8.41.

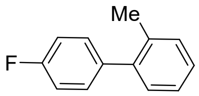

4’-fluoro-2-methyl-1,1’-biphenyl

^{1}H NMR (500 MHz, $CDCl_3$) δ 7.91 (d, 2H), 7.40 (d, 2H), 7.20(d, 1H), 7.10 (t, 1H), 7.07 (t, 1H), 7.01 (d, 1H), 2.90 (s, 3H)

^{13}C NMR (126 MHz, $CDCl_3$) δ 130.50, 125.11, 77.29, 77.04, 76.79, 45.56, 22.90, 7.94.

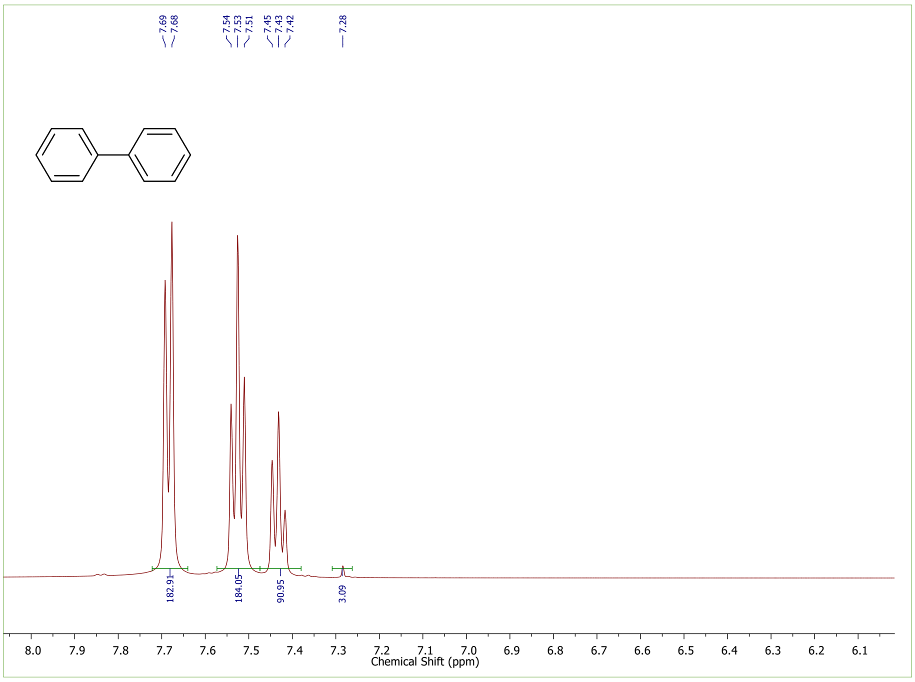

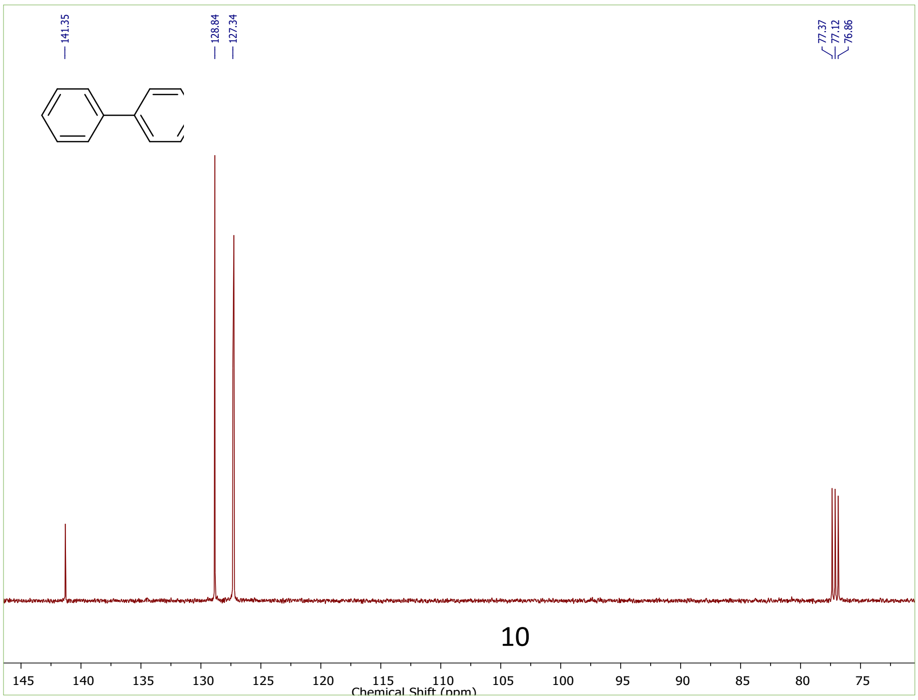

Figure S3: ^{1}H and ^{13}C NMR spectra of biphenyl.

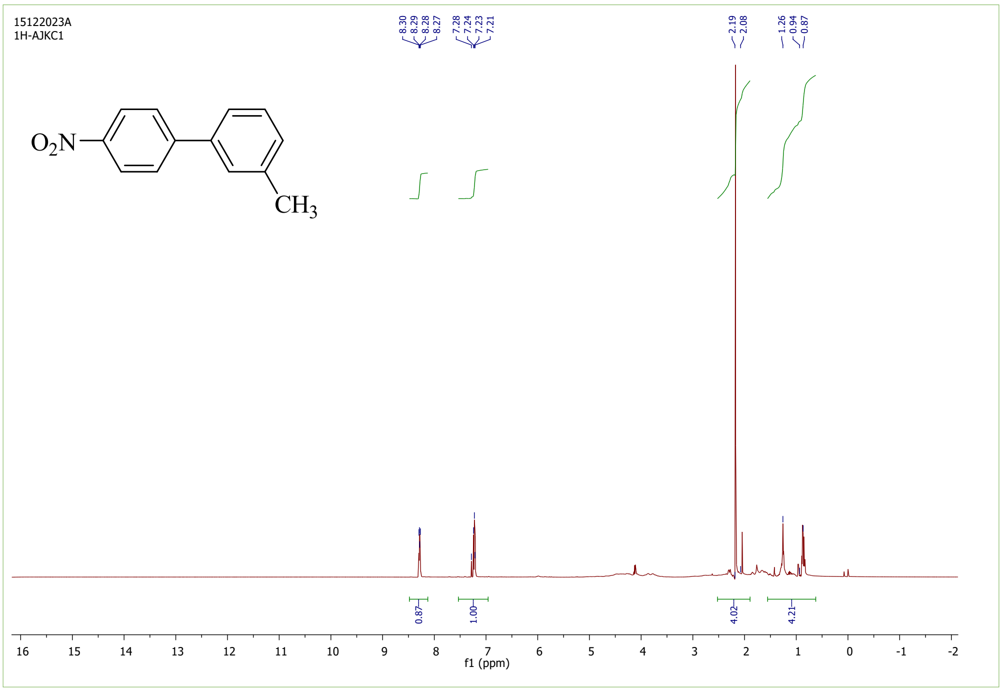

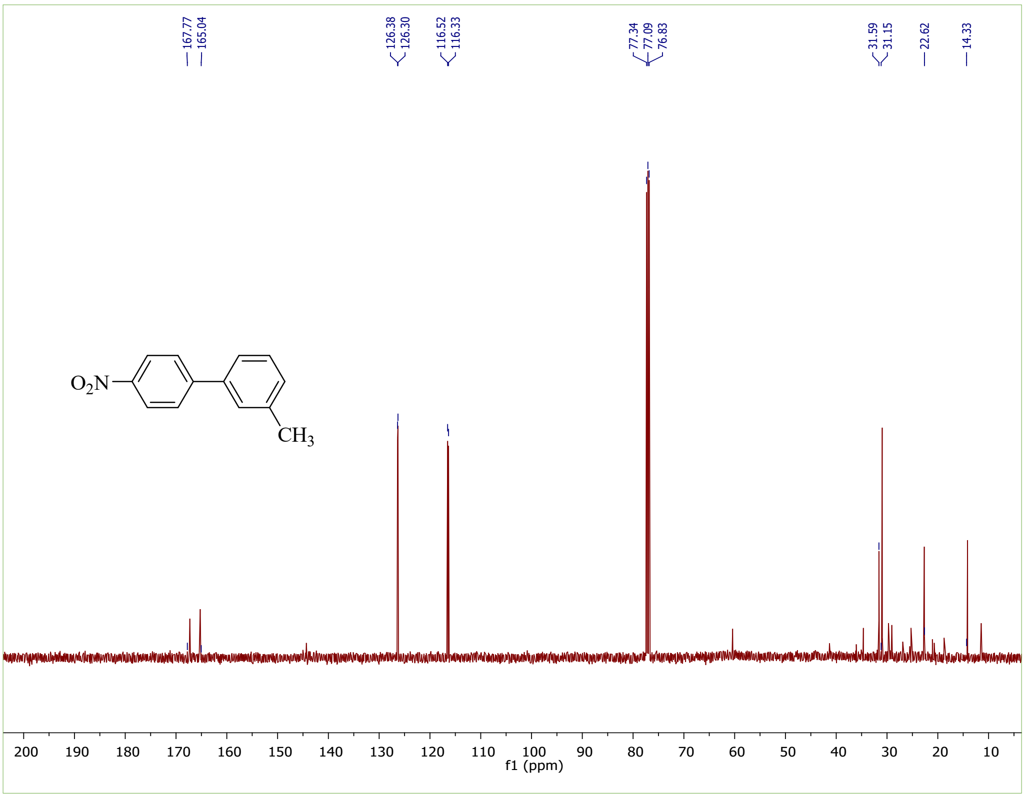

Figure S4: ^{1}H and ^{13}C NMR spectra of 3-Methyl-4′-nitro-biphenyl.

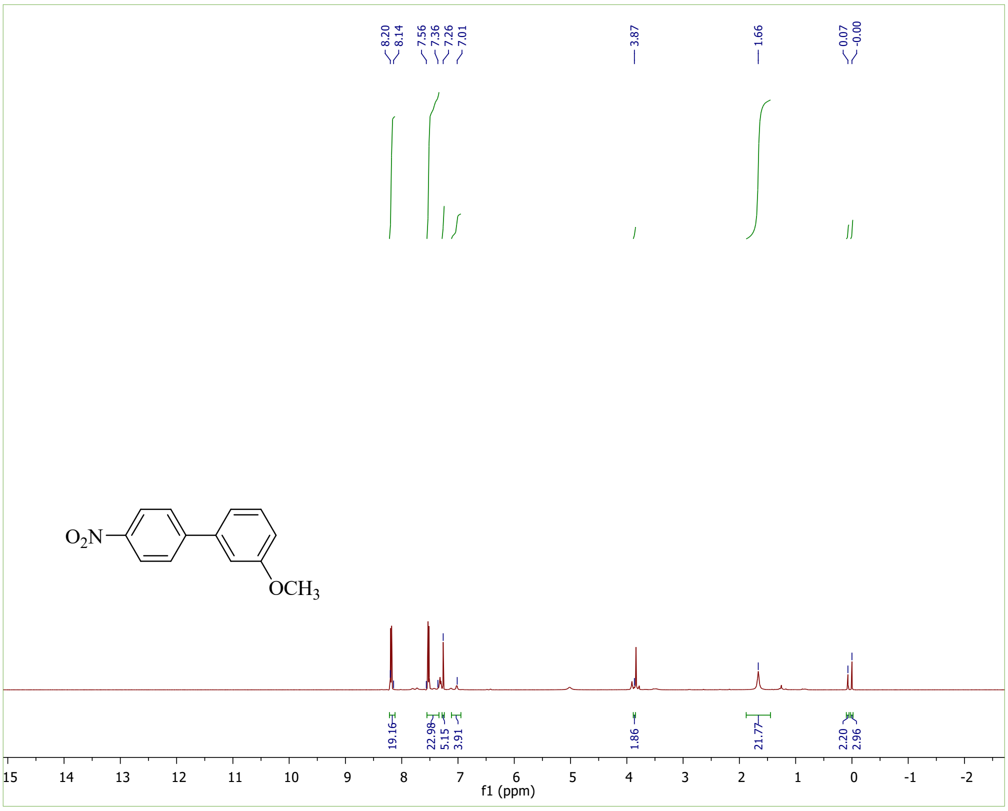

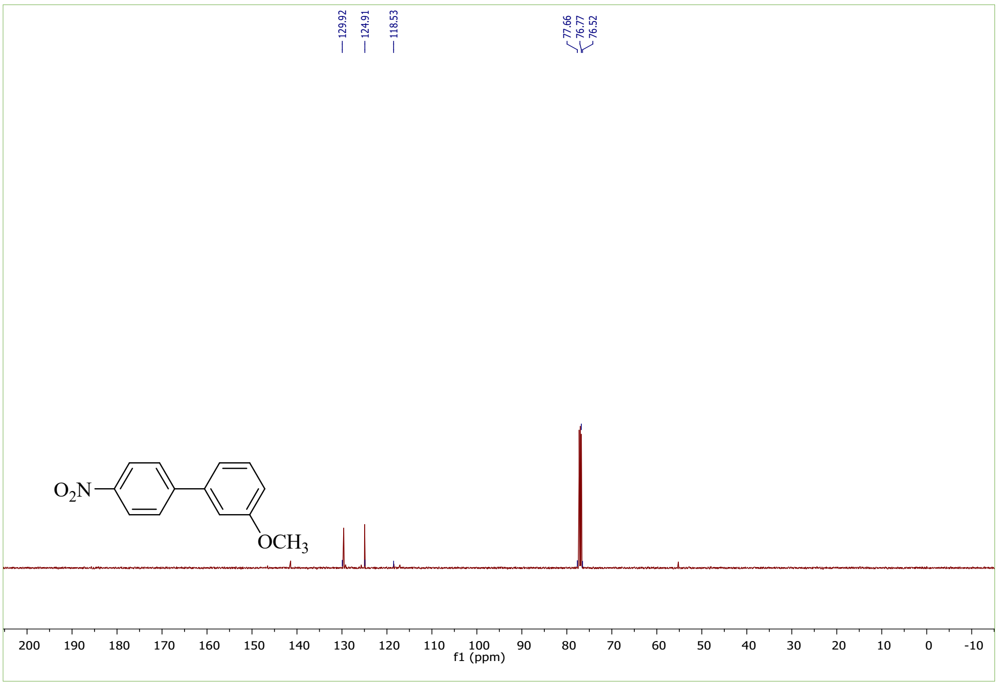

Figure S5: ^{1}H and ^{13}C NMR spectra of 3-Methoxy-4′-nitro-biphenyl.

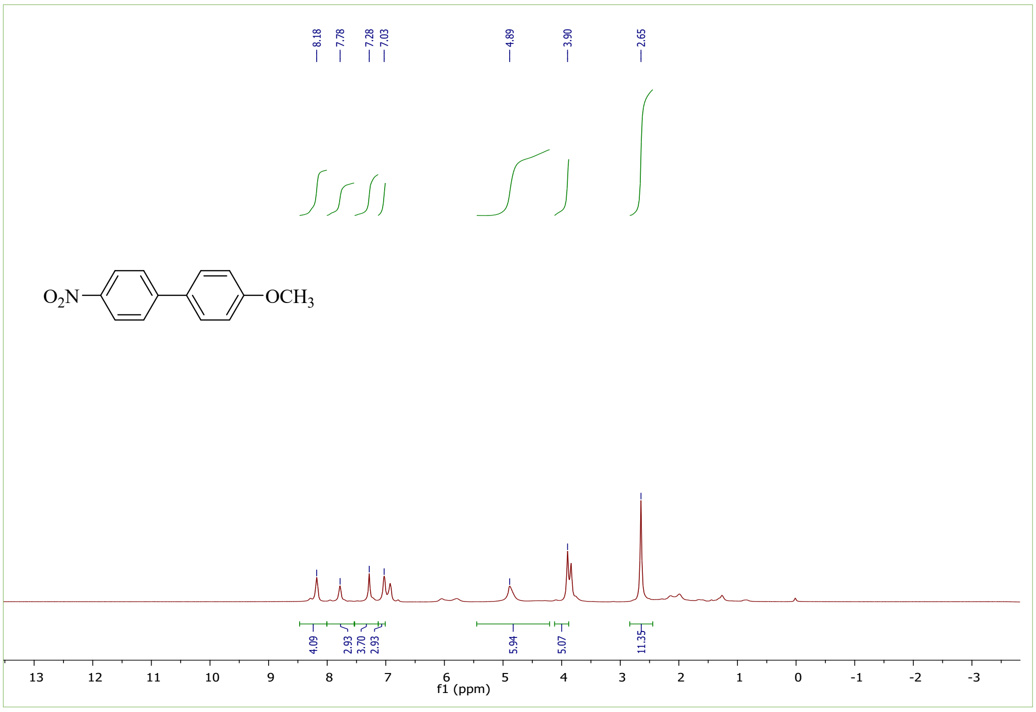

.

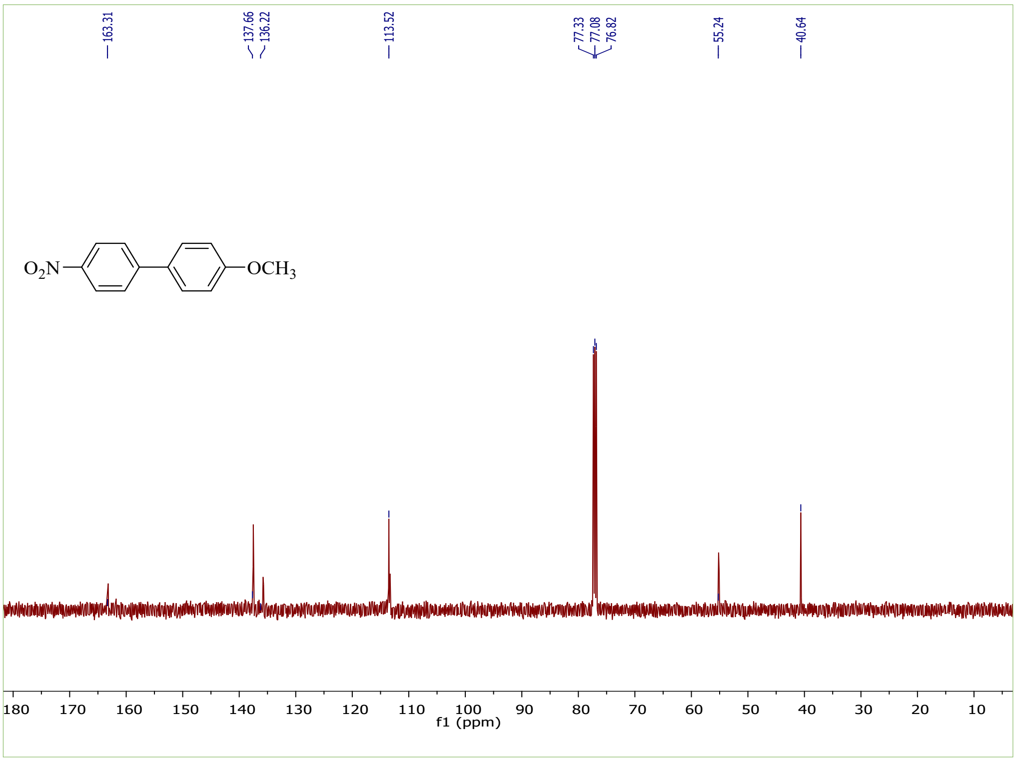

Figure S6: ^{1}H and ^{13}C NMR spectra of 4-Methoxy-4′-nitro-biphenyl.

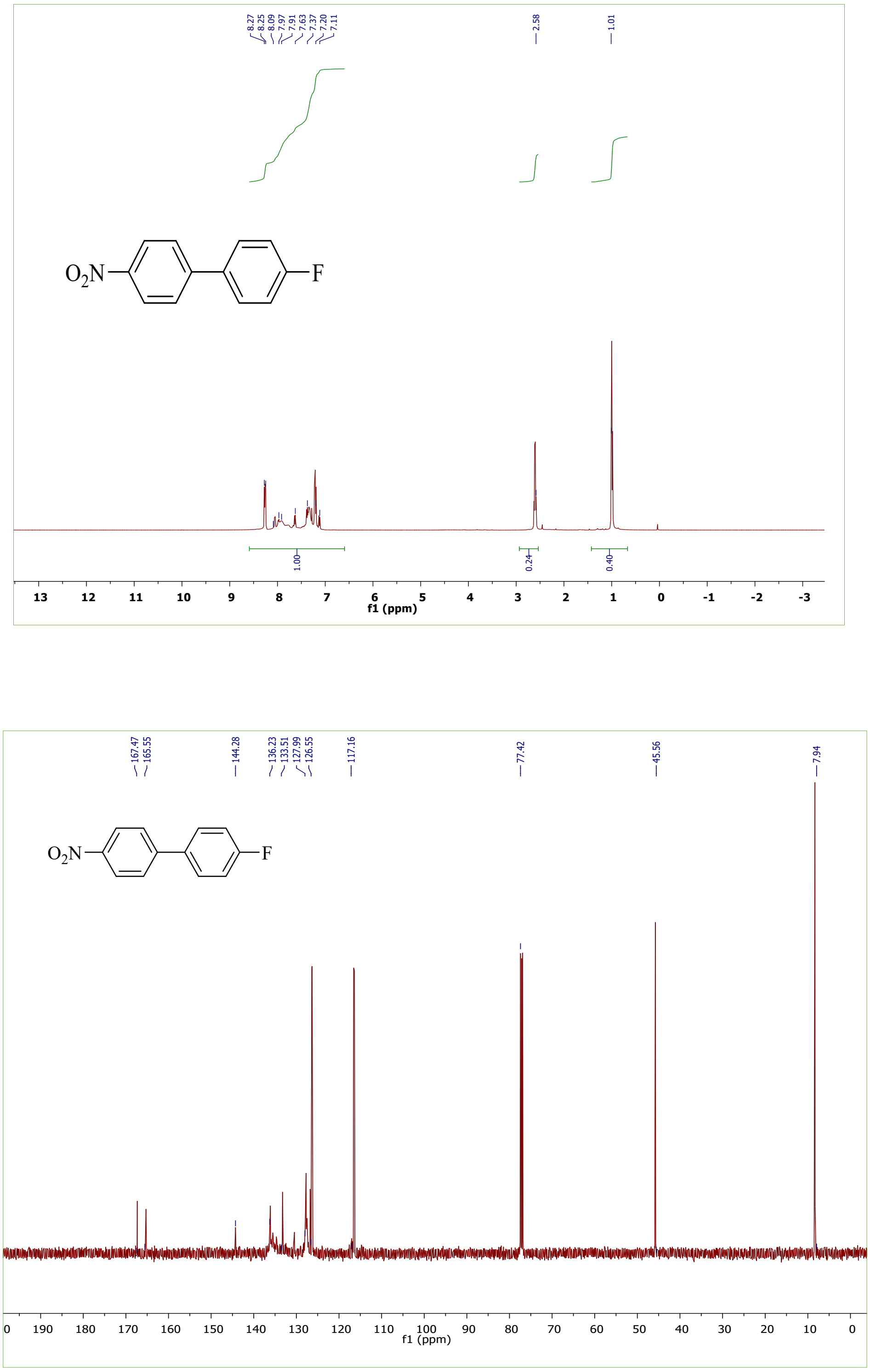

Figure S7: ^{1}H and ^{13}C NMR spectra of 4’--Fluoro-4-nitro-biphenyl.

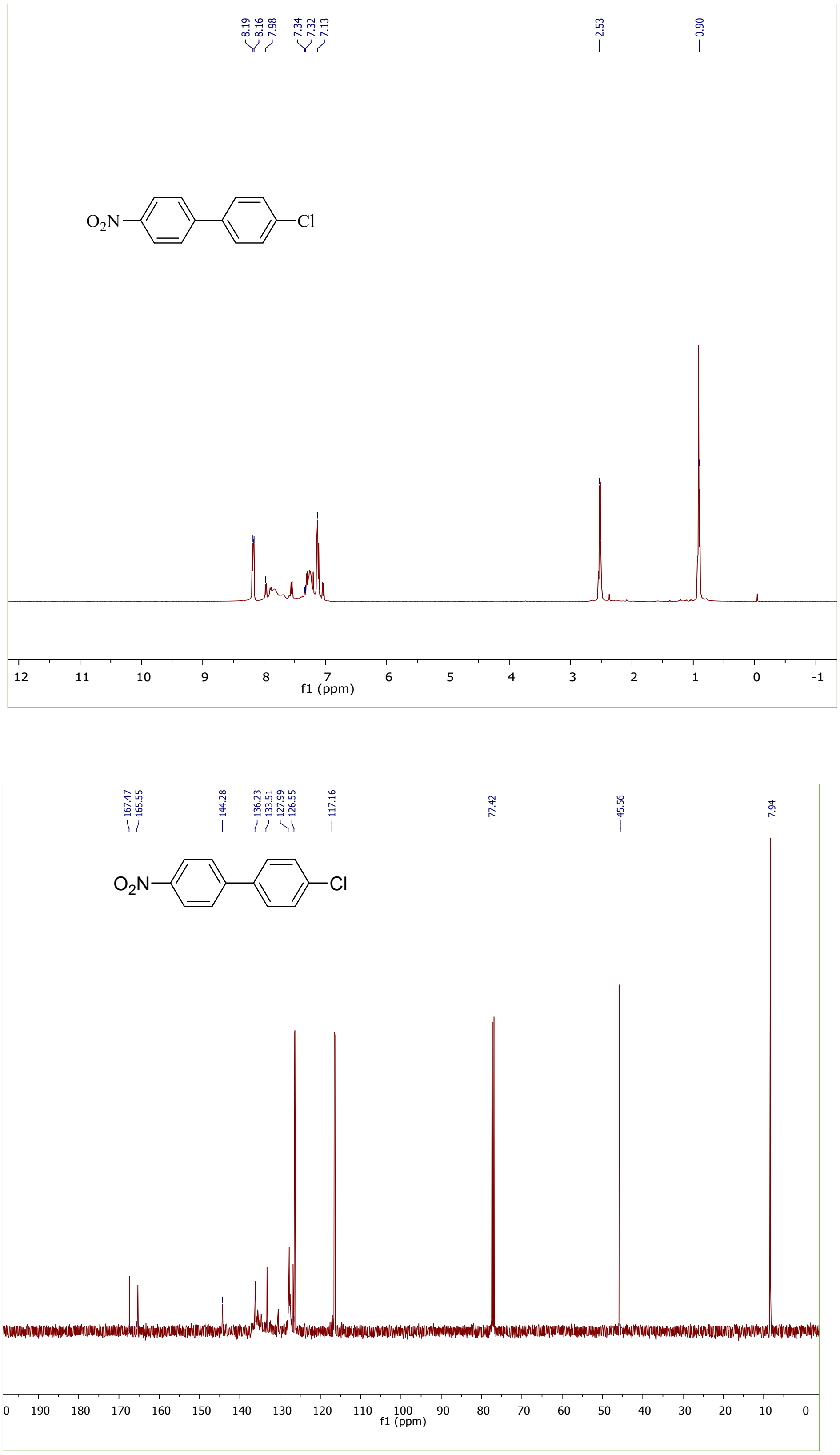

Figure S8: ^{1}H and ^{13}C NMR spectra of 4’-Chloro-4-nitro-biphenyl.

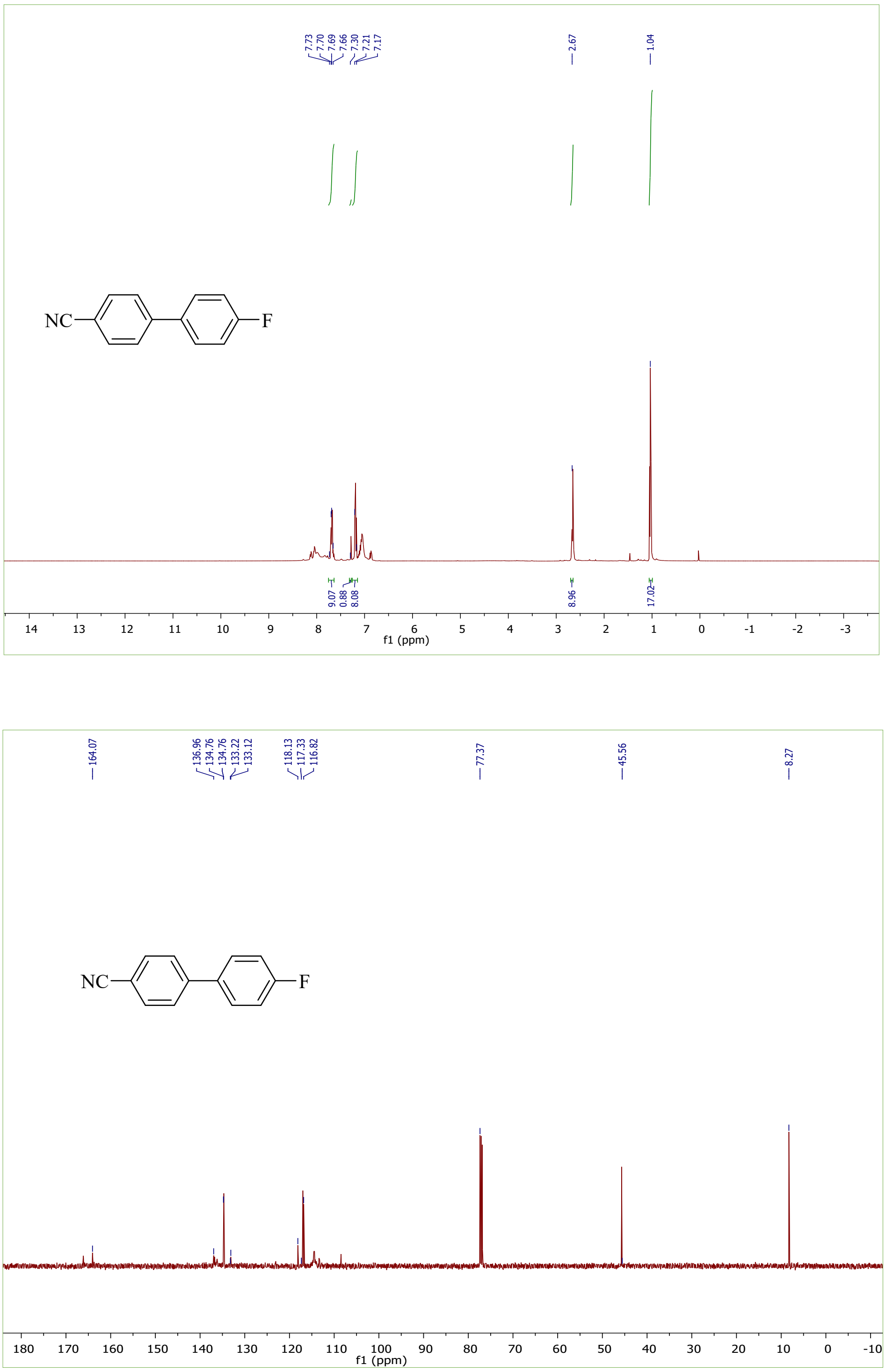

Figure S9: ^{1}H and ^{13}C NMR spectra of 4’-Fluoro-biphenyl-4-carbonitrile.

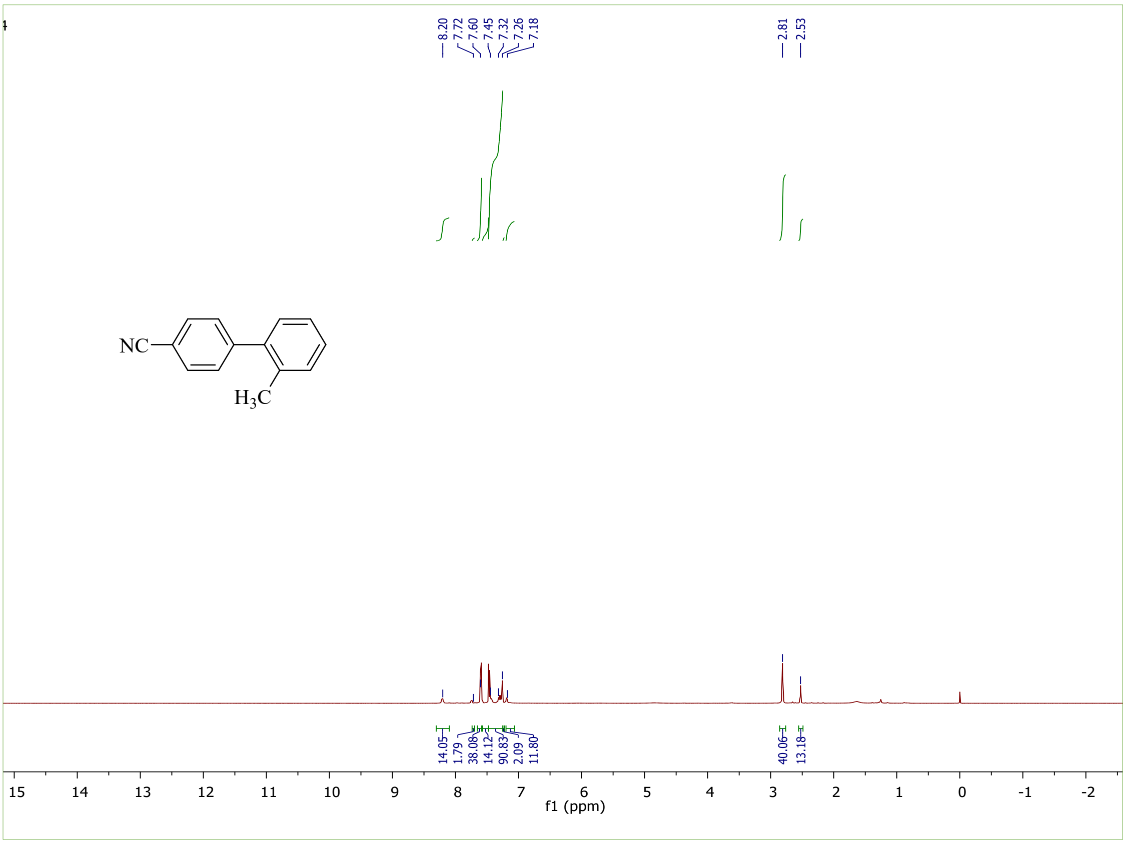
8.20
7.72
7.60
7.45
7.32
7.26
7.18
2.81
2.53
NC
H3C
14.05
1.79
38.08
14.12
90.83
2.09
11.80
40.06
13.18
15
14
13
12
11
10
9
8
7
6
5
4
3
2
1
0
-1
-2
f1 (ppm)

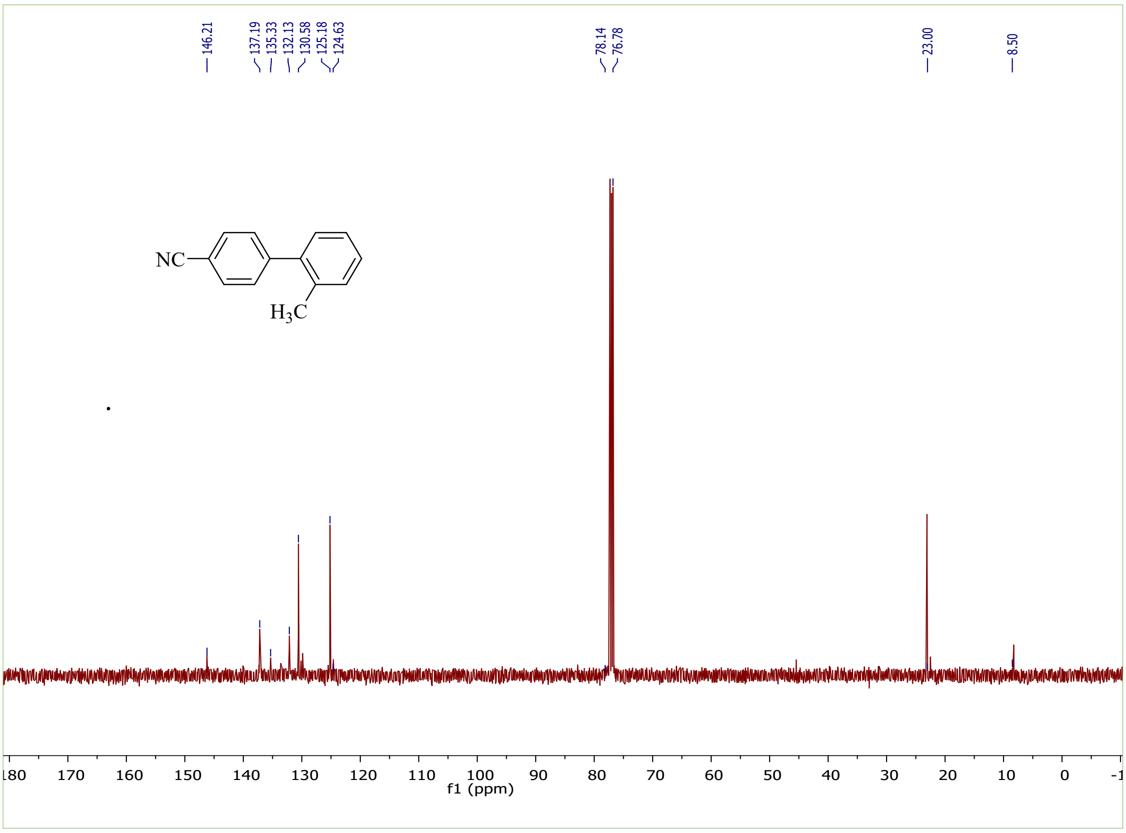
146.21
137.19
135.33
132.13
130.58
125.18
124.63
78.14
76.78
23.00
8.50
NC
H3C
180
170
160
150
140
130
120
110
100
90
80
70
60
50
40
30
20
10
0
f1 (ppm)

Figure S10: ^{1}H and ^{13}C NMR spectra of 2’-Methyl-biphenyl-4-carbonitrile.

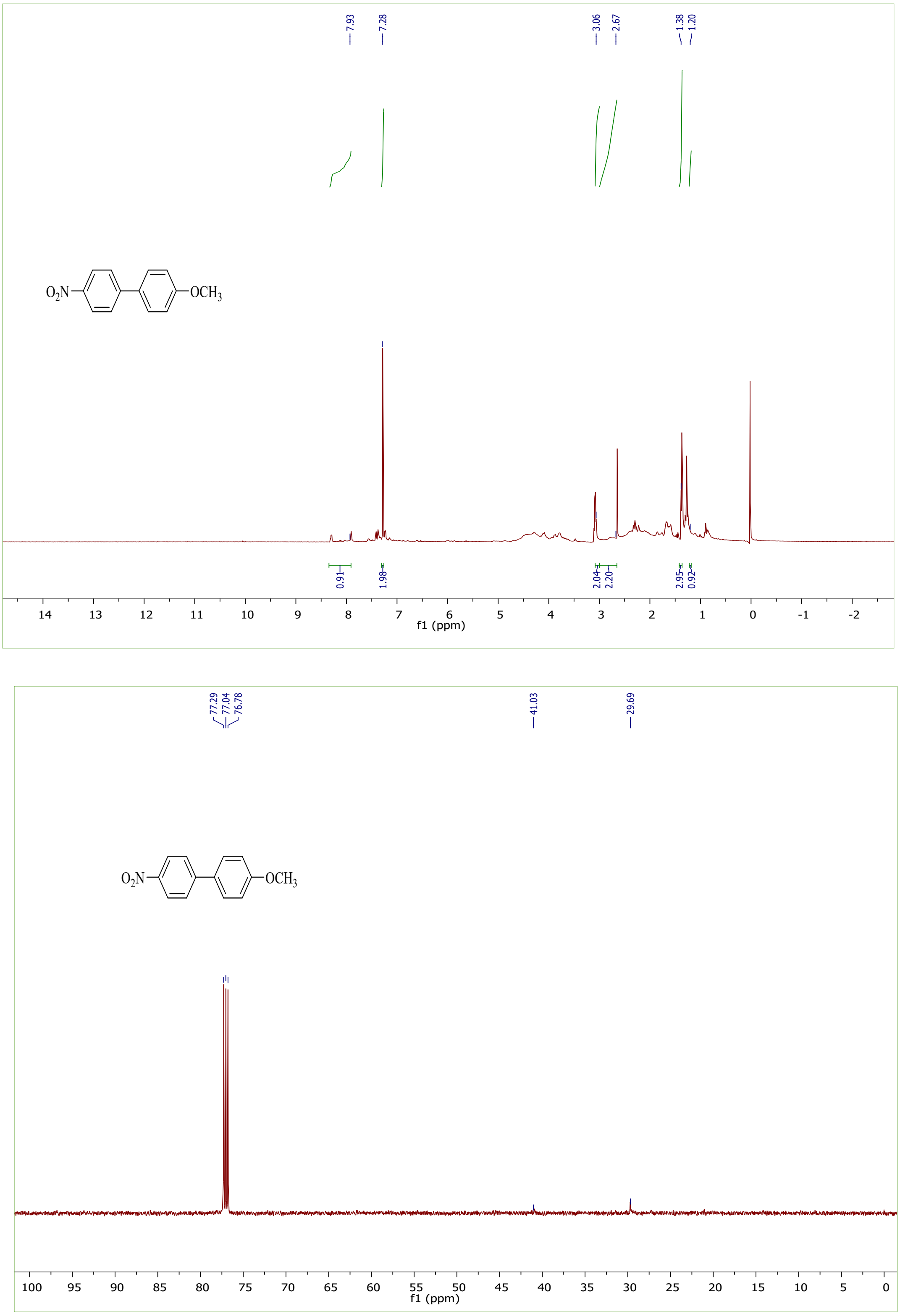

Figure S11: ^{1}H and ^{13}C NMR spectra of 4-(-3*H*-1λ^4-Thiophen-3-yl)-benzonitrile.

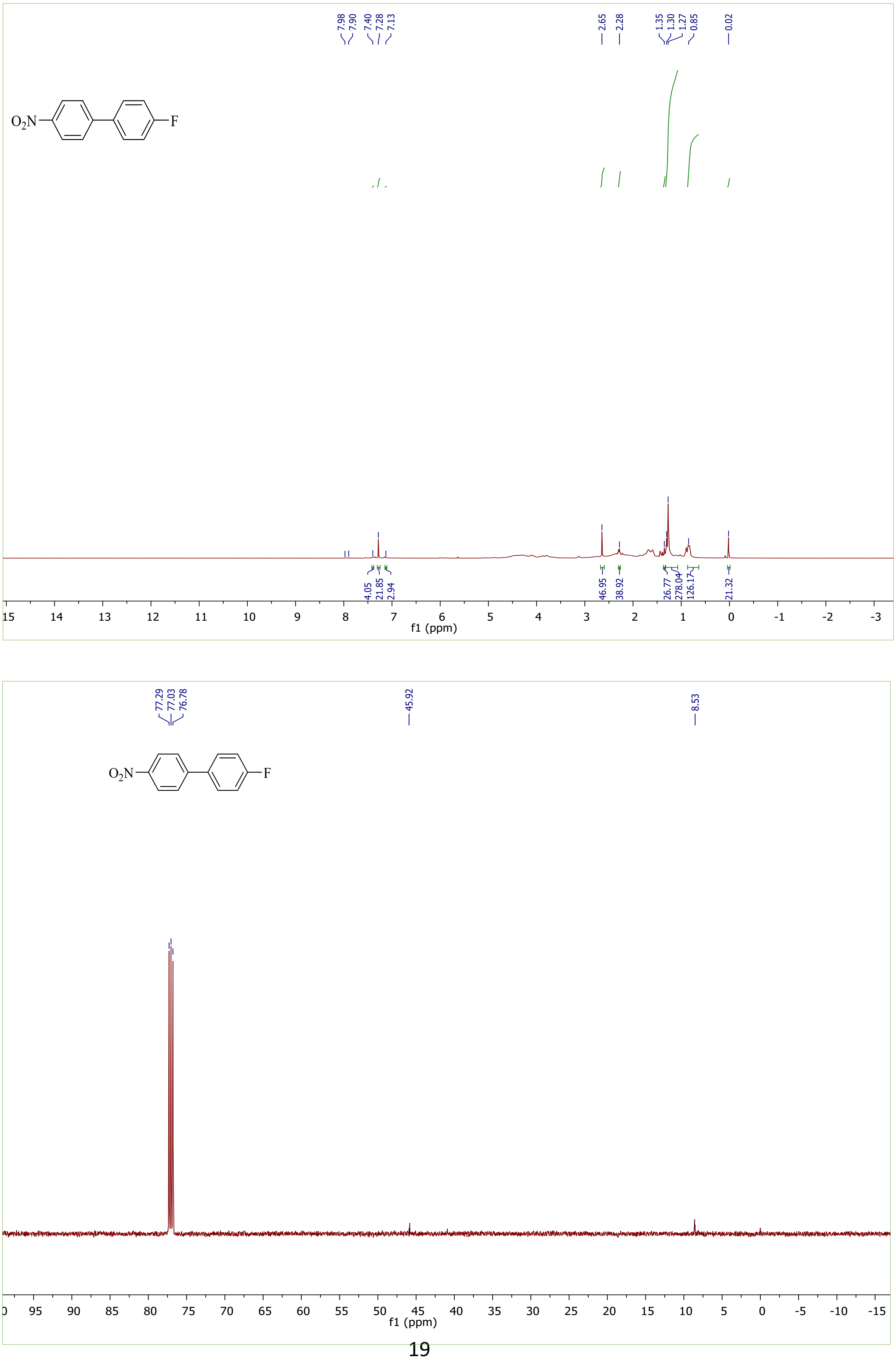

Figure S12: ^{1}H and ^{13}C NMR spectra of 3-(4-Nitro-phenyl)-3*H*-1λ^{4}-thiophene.

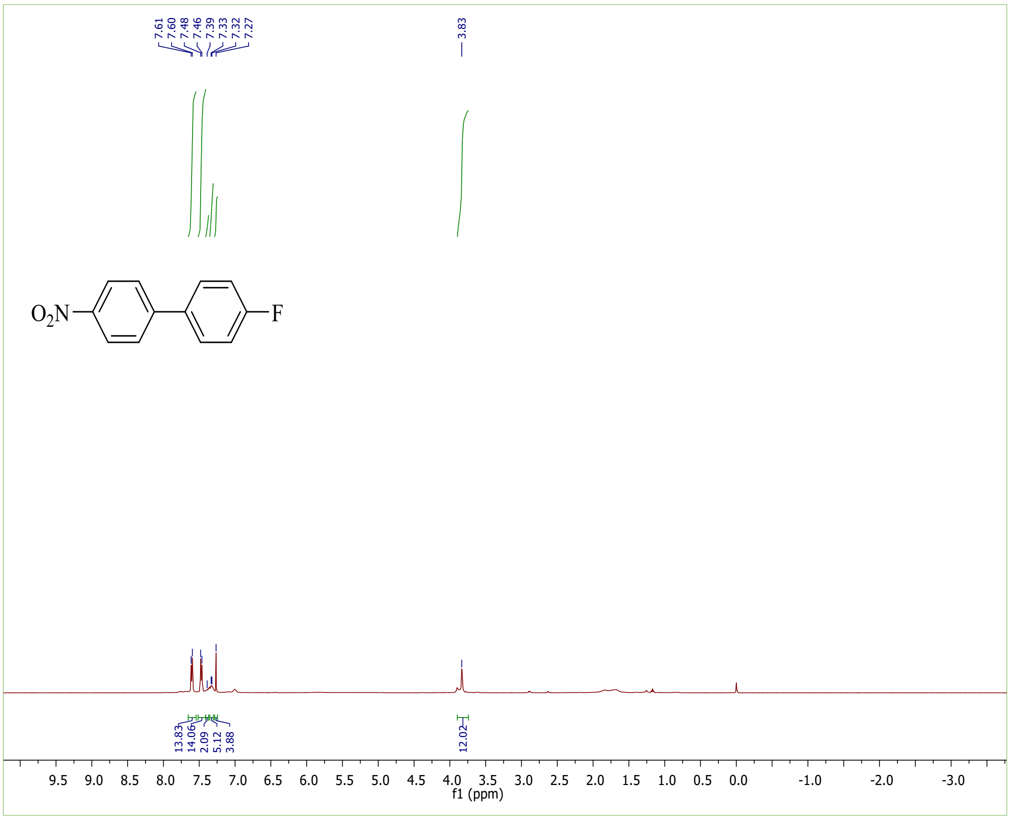

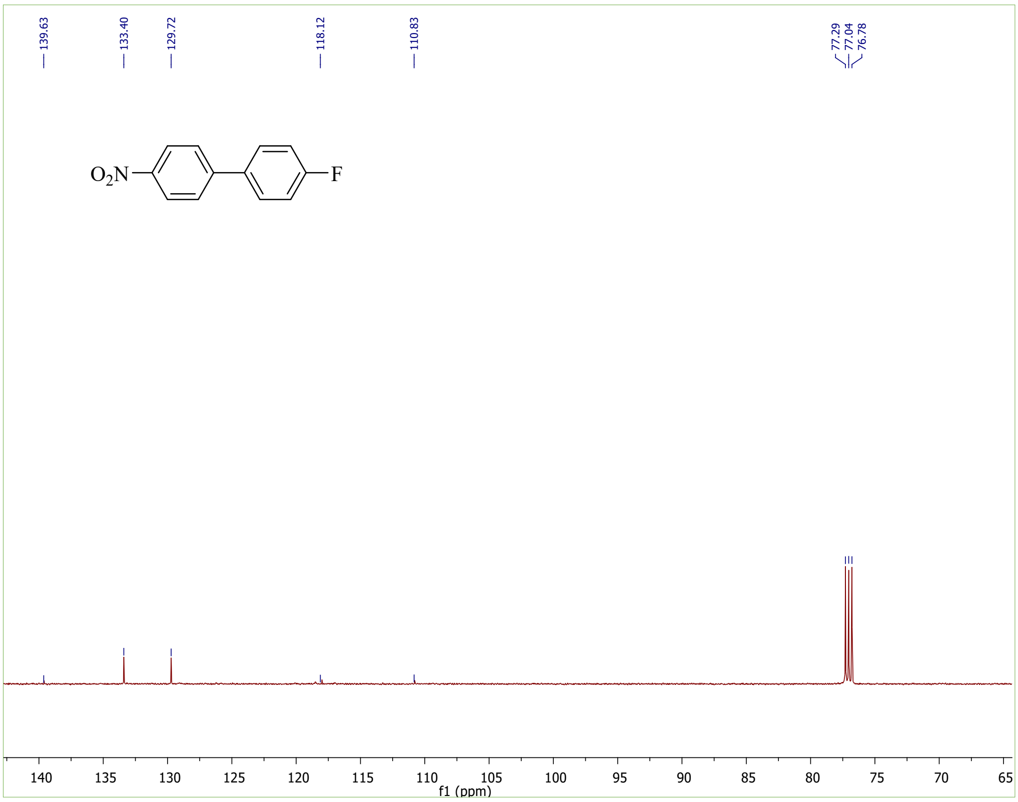

Figure S13: ^{1}H and ^{13}C NMR spectra of 3-Methoxy-4′-benzonitrile.

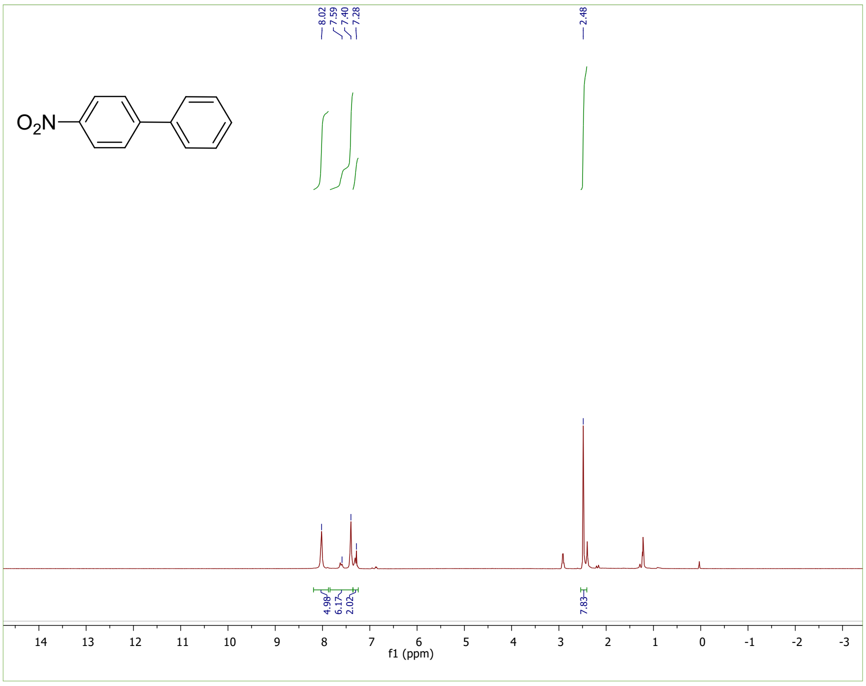

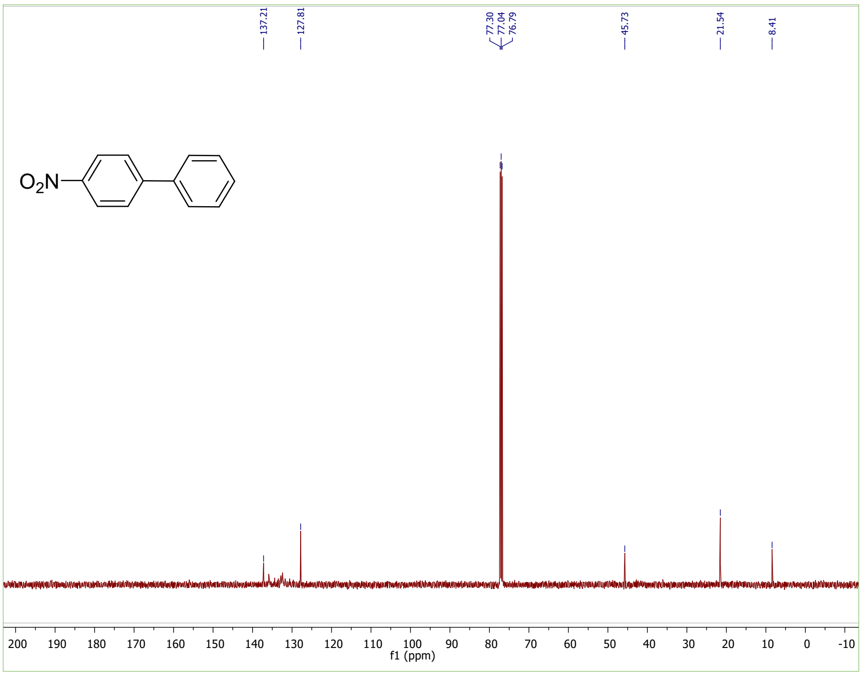

Figure S14: ^{1}H and ^{13}C NMR spectra of 2-(m-tolyl)pyridine.

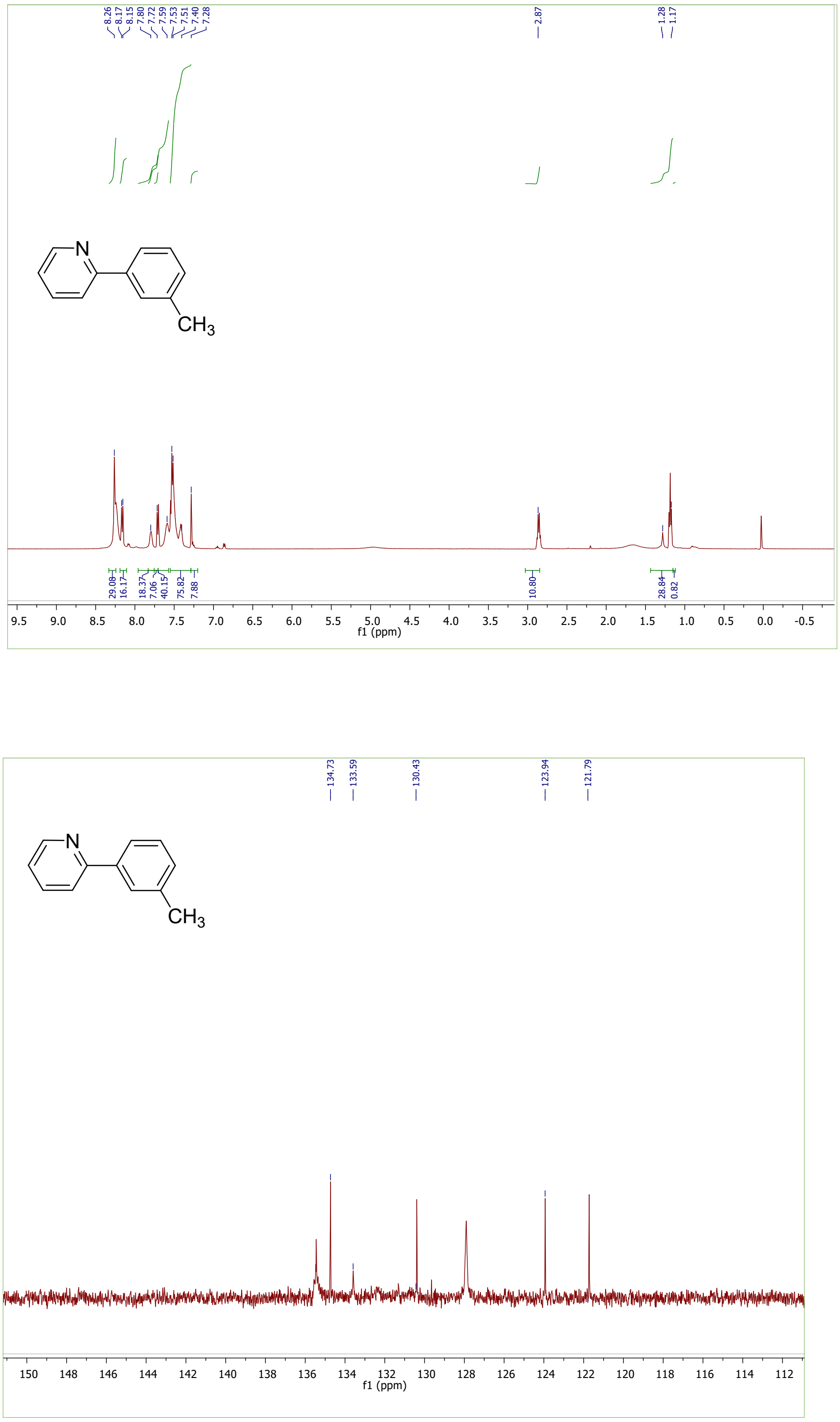

Figure S15: ^{1}H and ^{13}C NMR spectra of **4-nitro-1,1’-biphenyl**.

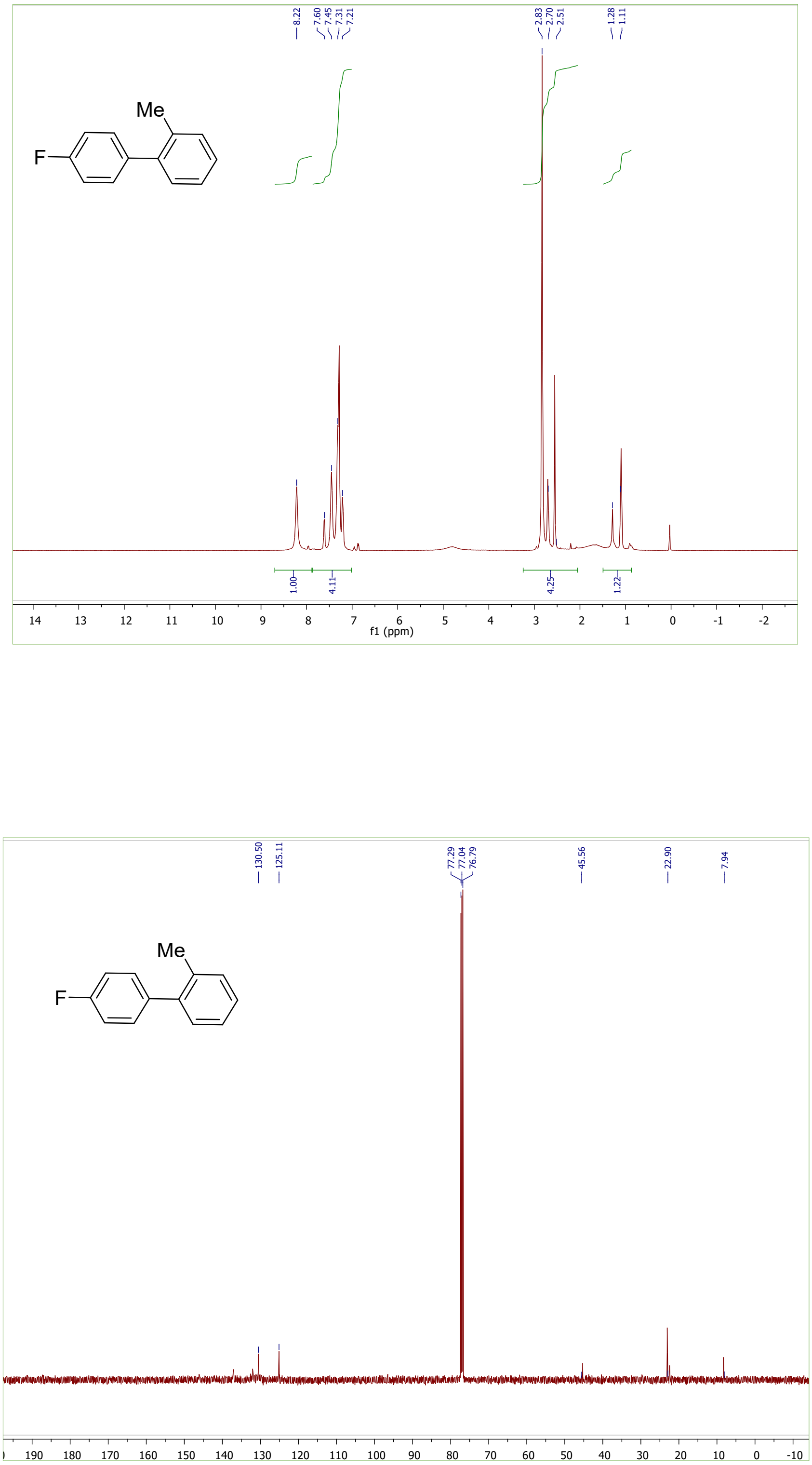

Figure S16: ^{1}H and ^{13}C NMR spectra of 4'-fluoro-2-methyl-1,1'-biphenyl.